

Thermo- and pH-Responsive Polymersomes of Poly(α,β -*N*-substituted-DL-aspartamide)s

Shih-Pin Hsu,¹ I-Ming Chu,^{1,2} Jean-Dean Yang³

¹Department of Chemical Engineering, National Tsing Hua University, Hsinchu, Taiwan 300, Republic of China

²Graduate School of Biotechnology and Bioengineering, Yuan Ze University, Taoyuan, Taiwan 320, Republic of China

³Material and Chemical Research Laboratories, Industrial Technology Research Institute, Taiwan, Republic of China

Received 11 March 2011; accepted 23 July 2011

DOI 10.1002/app.35348

Published online 16 December 2011 in Wiley Online Library (wileyonlinelibrary.com).

ABSTRACT: Materials that can respond to multiple stimuli, such as temperature and pH changes, are of considerable interest for applications in drug delivery systems. Notably, α,β -[poly(2-hydroxyethyl)-DL-aspartamide] is a potentially useful material for such applications. This study investigated the temperature and pH responsiveness of polymers structurally similar to α,β -[poly(2-hydroxyethyl)-DL-aspartamide], namely, poly(α,β -*N*-substituted-DL-aspartamide)s, in aqueous media. These polymers were derived from polysuccinimide (PSI), which was first synthesized via acid-catalyzed bulk polycondensation of L-aspartic acid (L-ASP) in the presence of 85% *o*-phosphoric acid under N₂. Two primary amino alcohols, 4-aminobutanol (4AB) and 6-aminohexanol (6AH), were then respectively utilized to modify PSI to form poly(α,β -*N*-substituted-DL-aspartamide)s via aminolysis. Different ratios of these two amino alcohols were used to modify

the polymer to produce a series of copolymers with lower critical solution temperatures ranging from 53–28°C when dispersed in aqueous media. Moreover, the properties of the poly(α,β -*N*-substituted-DL-aspartamide)s in aqueous solution were affected by pH changes. The morphology of the particles formed by these amphiphilic polymers was observed using scanning electronic microscopy and transmission electronic microscopy, and the particles were found to be polymersomes with shell and hollow core structures and diameters of 0.5–1 μ m. Other properties of this series of self-assembly copolymers were also characterized. © 2011 Wiley Periodicals, Inc. *J Appl Polym Sci* 125: 133–144, 2012

Key words: copolymers; drug delivery systems; polycondensation; self-assembly; transmission electronic microscopy

INTRODUCTION

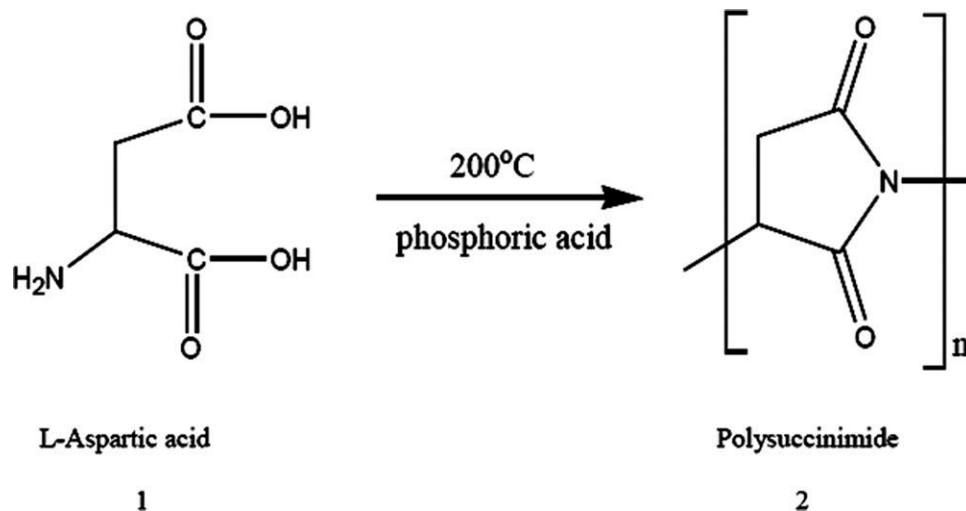
External stimuli,^{1–3} such as light,⁴ electrical current,⁵ chemicals,⁶ temperature,^{7–11} and pH,^{12,13} can trigger distinct and sudden changes in the shape, solubility, or self-assembly mode in “intelligent” or “smart” polymers.^{1–3} These materials can be used in drug delivery, biosensors, and tissue engineering.^{14–16} To develop these applications, the relationship between the structure and properties of environmental sensitive materials must be investigated comprehensively. Many such studies have been conducted in recent years.^{17–22} Materials that respond to single, dual, or multiple stimuli have been designed via graft modification or copolymerization of hydrophilic and hydrophobic segments.^{10,23–26} For example, temperature-sensitive materials, such as mPEG-PLGA⁹, poly

(*N*-vinyl caprolactone),^{27,28} poly (NiPAAm),²⁸ poly (siloxo ethylene glycol),^{28,29} poly (*N*-vinyl isobutyramide),³⁰ and polyphosphazene,^{31,32} can change from transparent to opaque and even be precipitated out as temperature increases. The temperature of the transition is called the lower critical solution temperature (LCST); this transition is due to the imbalance of the intermolecular forces between the polymer and the solvent and between the polymer molecules. On the basis of free energy theory ($\Delta G = \Delta H - T\Delta S$), the enthalpy term (ΔH) dominates below the LCST, whereas the entropy term (ΔS) dominates above the LCST.^{31–41} At low temperature,¹⁰ H-bonding interactions between polar groups and water lead to good solubility of the polymers. The water surrounding the nonpolar groups is in a low entropic state relative to free water, leading to an entropic penalty. As the nonpolar surface area of the polymer increase, this entropic penalty increases, causing the LCST to decrease. That is, favorable interactions below the LCST via hydrogen bonding between the amide groups in polymers and water molecules lead to dissolution of polymer chains. Above the LCST, hydrogen bonds are broken, and water molecules are expelled from the polymer, resulting in polymer precipitation.^{16,42}

Additional Supporting Information may be found in the online version of this article.

Correspondence to: I. Chu (imchu@che.nthu.edu.tw).

Contract grant sponsor: National Science Council, Taiwan, Republic of China; contract grant number: NSC 99-2221-E-007-007-MY2.

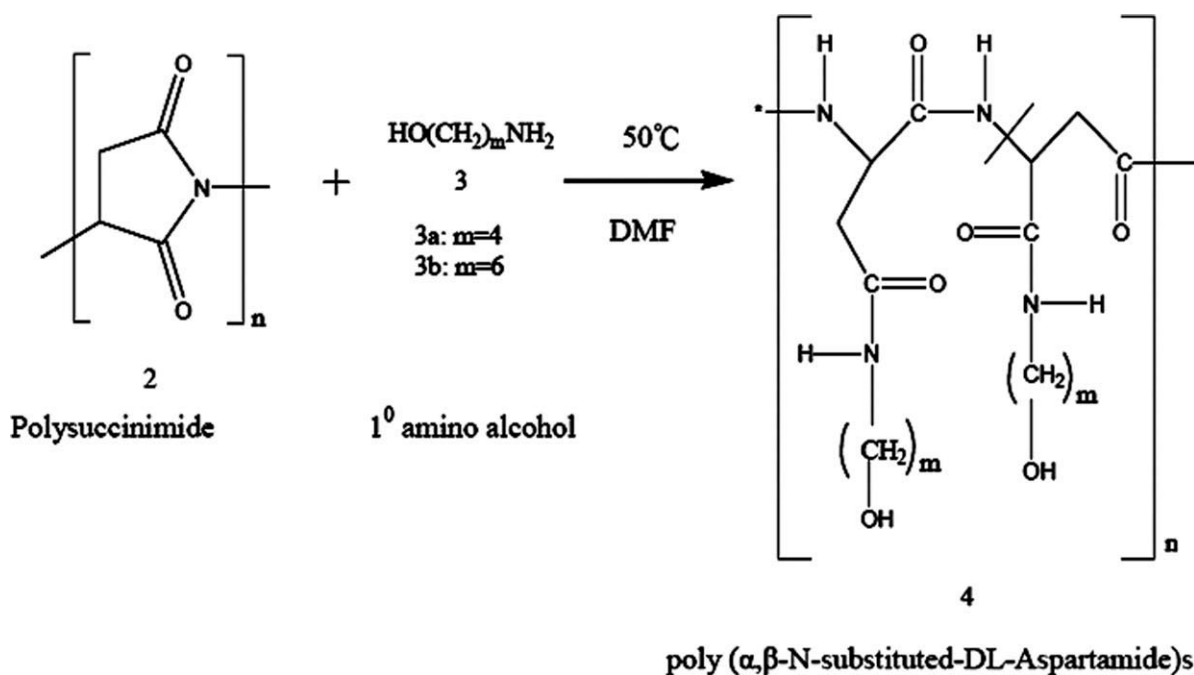


Scheme 1 Synthesis scheme of PSI.

The pH sensitivity of polymers has been determined to be the result of the interaction between the negatively charged groups of the polymer/solvent and the positively charged groups of the solvent/polymer. Polymers containing ionizable functional groups with a positive or negative charge that can change their charges according to pH are called pH-sensitive polymers.^{16,43,44} Most pH-sensitive polymers contain ionizable functional groups, such as poly(methacrylic acid)⁴³ and poly(acrylic acid) (PAA),⁴⁴ or are polyelectrolytes, such as poly(L-histidine),⁴⁵ poly(silamine)^{16,46} and poly(4-vinyl pyridine) (P4VP).¹⁸ Generally, these polymers have separable acidic (e.g., a carboxylic acid or sulfonic acid) and alkaline groups

(e.g., ammonium salts) or separable proton acceptors and proton donors.¹⁸ Electrostatic repulsion results in an increase in the hydrodynamic volume of the polymers or hydrogen bonding forms between block polymers and the environment as the pH changes in the milieu, causing swelling or shrinkage of the polymer's conformation and thus affecting the solubility of the polymer.^{12,13,43-49} For example, the imidazole ring of poly(histidine) has one electron pair on an unsaturated nitrogen that renders poly(histidine) amphiphilic by protonation-deprotonation.⁴⁵ The solubility of a material depends on the pH.⁴⁵

Among the temperature- and pH-sensitive polymers, PNiPAAm-PAA,¹⁰ poly(*N,N*-dimethylaminoethyl

Scheme 2 Synthesis scheme of poly(α,β -*N*-substituted-DL-aspartamide)s.

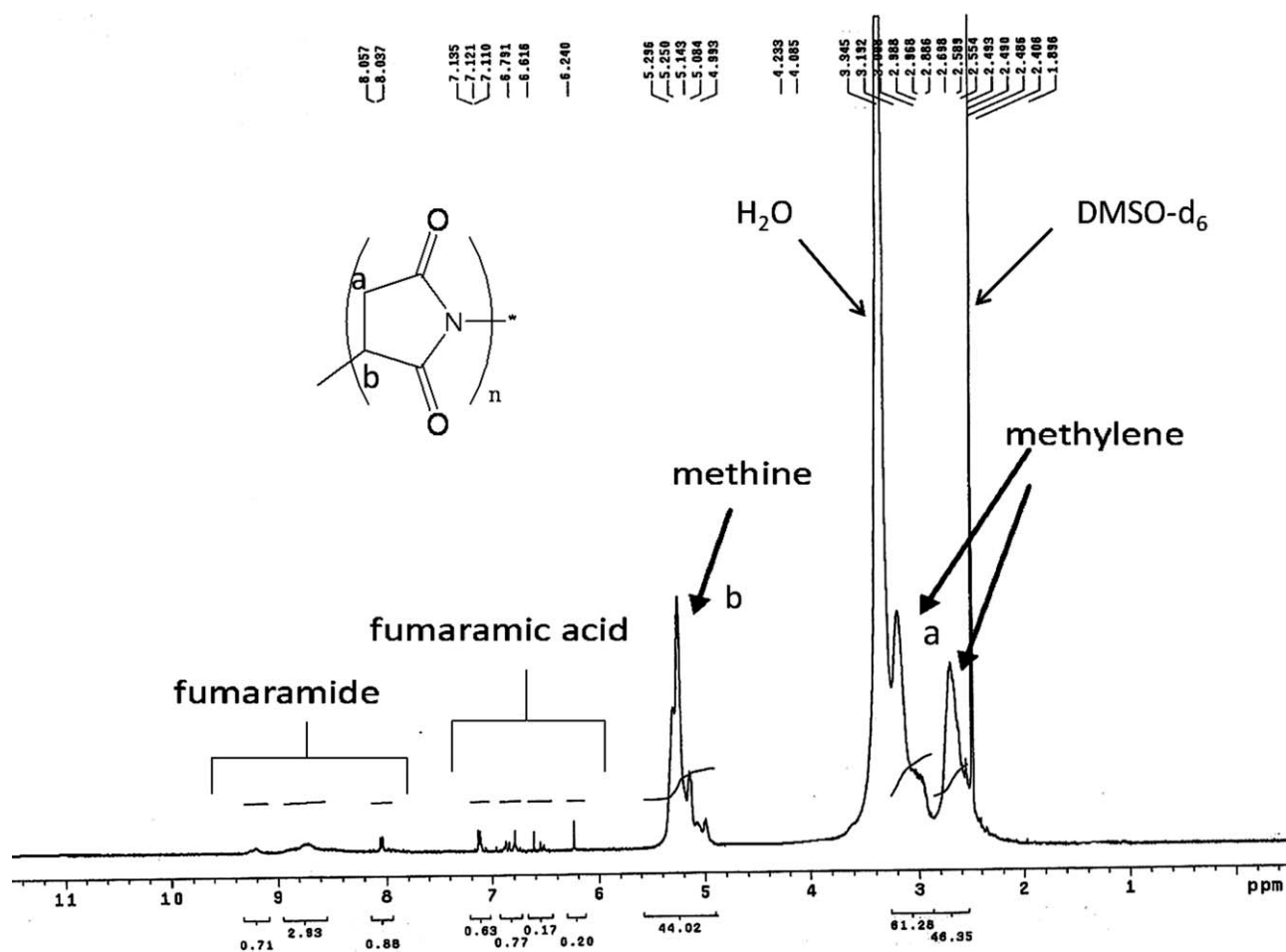


Figure 1 ¹H NMR (500 MHz, DMSO-d₆) spectra of the PSI obtained from bulk thermal polycondensation.

methacrylate),¹⁸ poly(*N*-acryloyl-*N*-propylpiperazine),²³ and poly(dichlorophosphazene),⁵⁰ (γ -PGA)-*b*-P(NiPAAm)⁵¹ have both pH- and temperature-sensitive properties. However, most stimuli-responsive polymers are not biodegradable, and some are even toxic.^{52–56} The development of biodegradable and

biocompatible stimuli-responsive polymers has become increasingly important in recent years.^{9,52–59} Therefore, searching for biodegradable/biocompatible materials with indications of temperature and pH sensitivity is a reasonable task in the development process. Poly(amino acid)s, such as poly(γ -glutamic acid) (γ -PGA), and poly(aspartic acid) (PASP), which have amide linkages and are thus peptides, are completely biodegraded by hydrolysis and are biocompatible.^{52–56,58–65} Although, γ -PGA and PASP were studied a couple of decades ago,⁶⁵ modified γ -PGA and PASP have been characterized only recently. For example, poly(α,β -*N*-substituted γ -glutamine)⁵² and

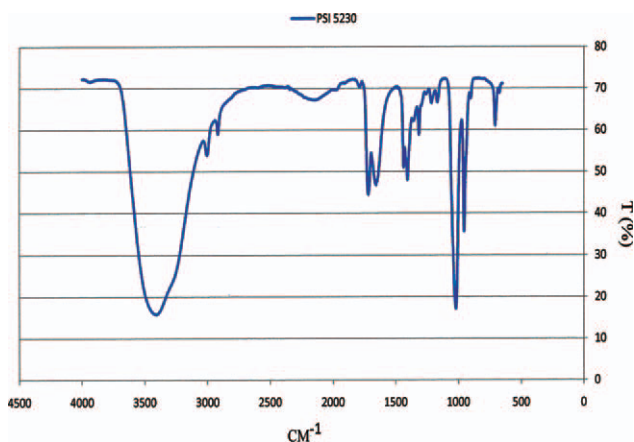


Figure 2 FTIR of PSI compared with the Fig. 6 and the difference can be distinguished between PSI and 1° amino alcohol modified PSI. [Color figure can be viewed in the online issue, which is available at wileyonlinelibrary.com.]

TABLE I
GPC Results (M_n (g/mol), M_w (g/mol), MP (g/mol), PdI) and DSC (T_g (°C), T_m (°C), ΔH (J/g)) and TGA (°C) of PSI

PSI			
M_n	2763	T_g	47.84
M_w	5230	T_m	110.86
MP	4587	ΔH	152.1116
PdI	1.89	TGA	400

MP, The peak of molecular weight.

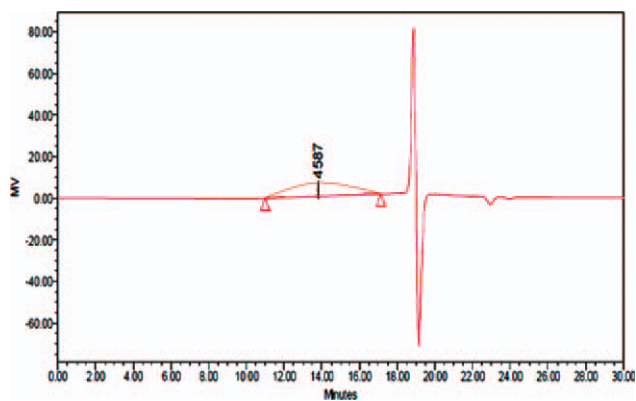


Figure 3 GPC diagram of PSI measured in DMF containing 20 mmol L^{-1} LiBr (Waters USA). [Color figure can be viewed in the online issue, which is available at wileyonlinelibrary.com.]

poly(*N*-substituted α/β -asparagine)s⁵³ are both temperature and pH responsive, as well as being biodegradable and biocompatible. Applying their unique physicochemical properties in drug and gene delivery systems has garnered considerable attention.^{52-56,58-60} However, large-scale production of poly(α,β -*N*-substituted γ -glutamine)s involves complex technical and economic problems. One basic requirement for production of a drug delivery carrier or biomaterial is simple and low-cost production.^{56,66}

Therefore, this study focused on further development of PASP-related materials. First, *L*-aspartic acid, which can be obtained either through chemical or biochemical processes⁶⁶ was used as the starting

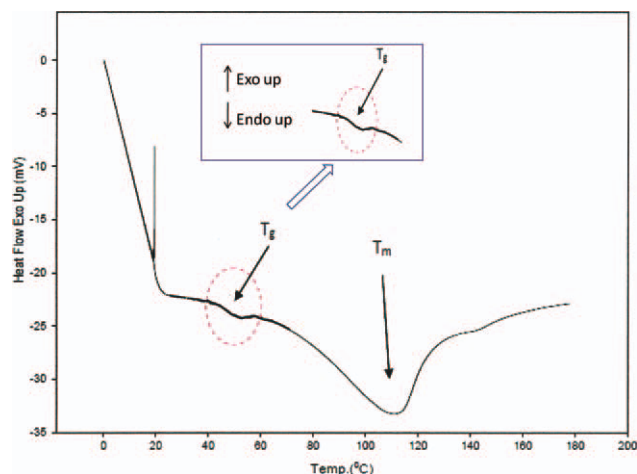


Figure 4 DSC diagram of PSI in the heating process $20^\circ\text{C}/\text{min}$. T_g , T_m can be found. [Color figure can be viewed in the online issue, which is available at wileyonlinelibrary.com.]

material to produce poly(succinimide) (PSI) by thermal bulk polycondensation.^{67,68} The PSI was then modified by grafting different ratios of primary amino alcohols, 4-aminobutanol (4AB) and 6-amino-hexanol (6AH), onto the succinimide ring to obtain novel poly(*N*-substituted α/β -aspartamide)s. The copolymers obtained contained both hydrophilic and hydrophobic segments together with ionizable groups. These copolymers formed self-assembled aggregates in an aqueous solution, and their properties changed in response to temperature or pH

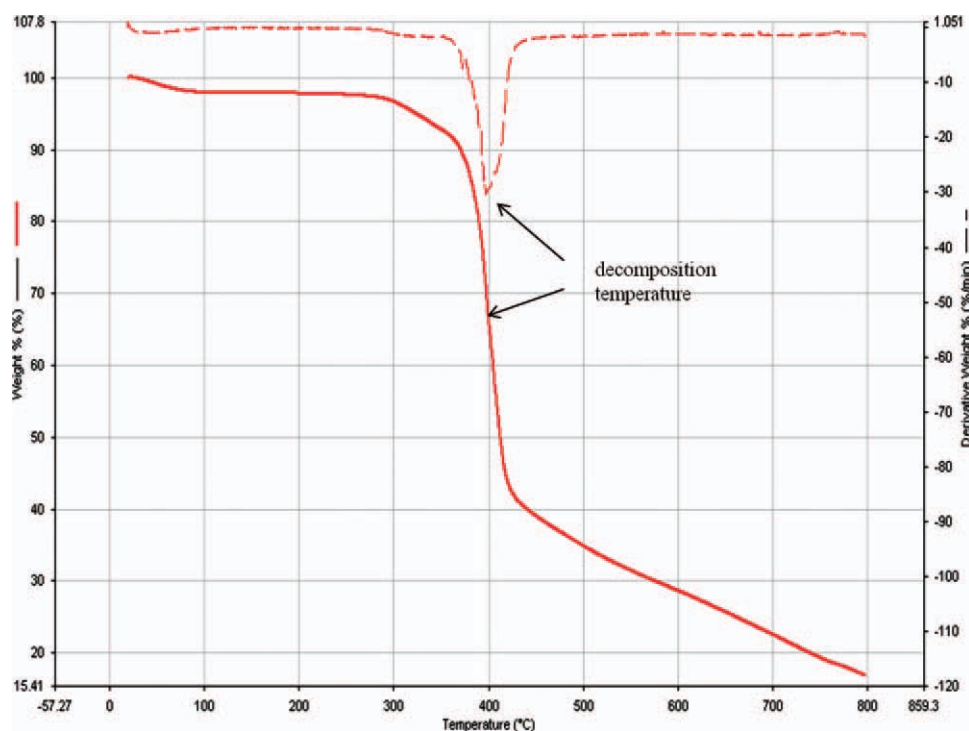


Figure 5 TGA diagram of PSI, the decomposition temperature can be found from the diagram. [Color figure can be viewed in the online issue, which is available at wileyonlinelibrary.com.]

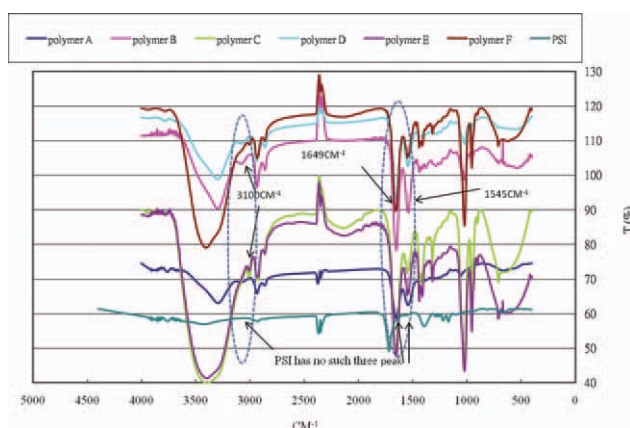


Figure 6 FTIR diagram of PSI and polymer A–F. The difference can be distinguished at three peaks shown in diagram. [Color figure can be viewed in the online issue, which is available at wileyonlinelibrary.com.]

changes. The relationships between their properties and structure are discussed.

EXPERIMENTAL

Materials

L-aspartic acid (reagent grade, purity $\geq 98\%$) (Sigma, USA) was used as received. Eighty-five percent *o*-phosphoric acid (Showa, Japan), 4-aminobutanol

TABLE II
GPC (M_n (g/mol), M_w (g/mol), MP (g/mol), PDI) of poly(α,β -*N*-substituted-DL-aspartamides)

	M_n	M_w	MP	PdI
Polymer B	3806	6288	5582	1.64
Polymer C	3764	6251	5392	1.66
Polymer D	3789	6259	5562	1.65
Polymer E	4826	9629	7583	1.97
Polymer F	4764	9399	7540	1.97

(98% purity, Sigma-Aldrich, USA), 6-aminohexanol (97% purity, Sigma-Aldrich, USA), and *N,N*-dimethylformamide (DMF) (Riedel de Haen, Germany) were dried over a Molecular Sieve 1A prior to use. Phosphotungstic acid *n*-hydrate crystals were from J. T. Baker, Japan, and carbon-coated copper grid (200 mesh) was from Agar Scientific, England.

Poly(succinimide) synthesis (see Scheme 1)⁶⁶

L-ASP(1) (20 g, 0.1504 mol) and 85% *o*-phosphoric acid (2 g, 17.34 mmol) were mixed in a three-necked round-bottom flask equipped with a mechanical stainless steel stirrer and an N_2 inlet and were heated to 200°C under an N_2 atmosphere. After 30 min, the reaction mixture changed to a mixture of light-yellow powder and clumps. The reaction mixture was kept

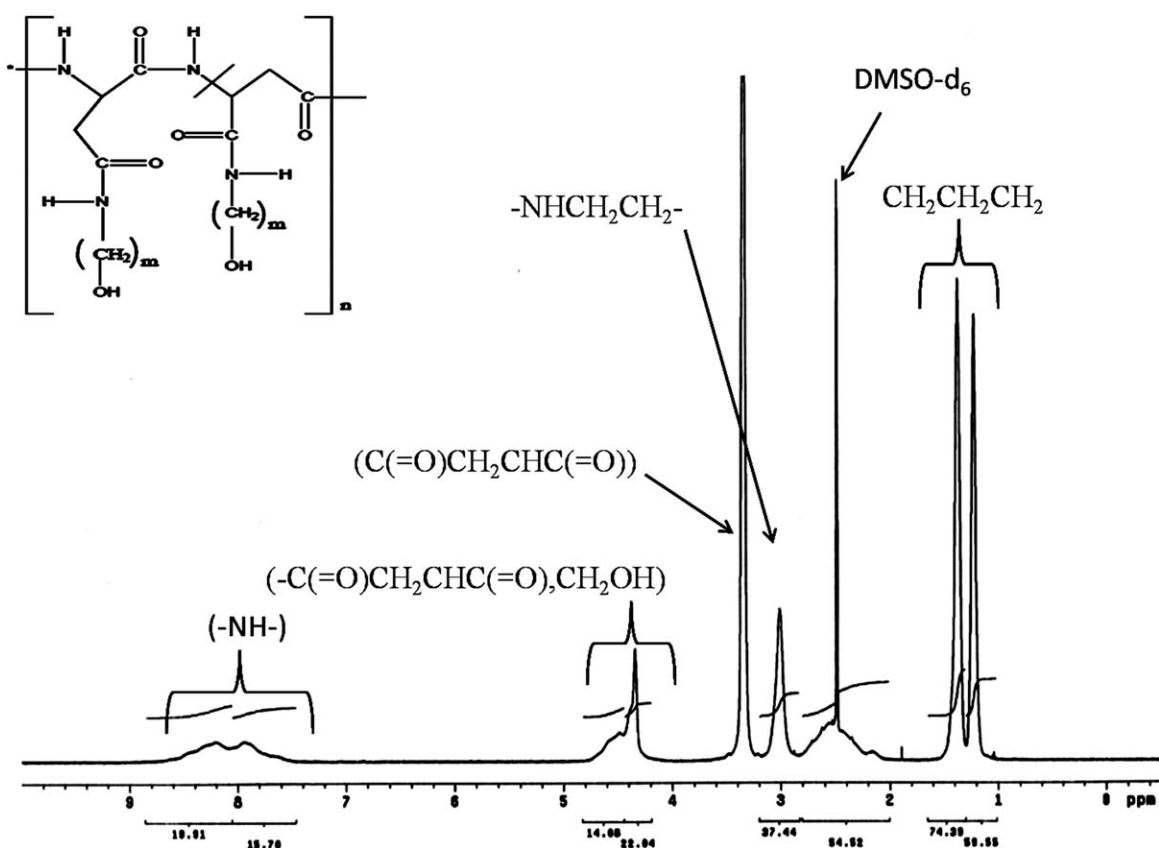


Figure 7 1H NMR (500 MHz, DMSO- d_6) of poly(α,β -*N*-substituted-DL-Aspartamide).

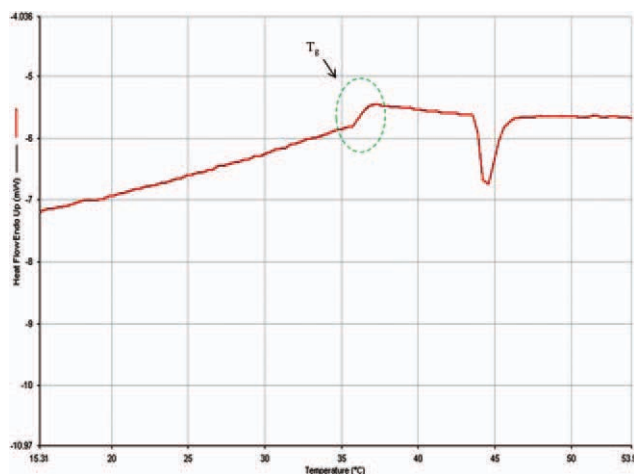


Figure 8 DSC diagram of poly(α,β -*N*-substituted-DL-Aspartamide) (polymer F) in the heating process 20°C/min. [Color figure can be viewed in the online issue, which is available at wileyonlinelibrary.com.]

at 200°C for 32 h. The product was washed with water (200 mL) for three times and followed by methanol (200 mL) for one time and then dried at 80°C under reduced pressure to yield PSI (2).

Synthesis of poly(α,β -*N*-substituted-DL-aspartamide)s (see Scheme 2)⁵³

Synthesis of (4) was carried out using PSI (1 g, 10.3 mmol) and an excess amount of a mixture of various amino alcohols (20.3 mmol) (molar ratio of PSI: a mixture of 1° amino alcohol = 1 : 2) at 50°C in anhydrous DMF under N₂ atmosphere for 4 h.

Upon completion of the reaction time, the products have been recovered by precipitation in ethyl ether, centrifuged, treated several times with acetone, dried under vacuum and purified by dispersing the dried products with R.O. water and then loading into a dialysis bag (MWCO 1000) to dialyze against a large amount of R. O. water; the water was changed daily for 1 week. The final product was obtained after lyophilization. The primary amino alcohols 4AB and 6AH were used as nucleophiles in the reaction. The following polymers with different amounts of 1° amino alcohol were synthesized: polymer A, 40% (8.12 mmol) 4AB and 60% (12.18 mmol) 6AH; polymer B, 30% (6.09 mmol) 4AB and 70% (14.21 mmol) 6AH; polymer C, 25% (5.075 mmol) 4AB and 75% (15.225 mmol) 6AH; polymer D, 20% (4.06 mmol) 4AB and 80% (16.24 mmol) 6AH; poly-

TABLE III
 T_g (°C) of Polymer B–F Measured by DSC

Polymer T_g (°C)				
Polymer B	Polymer C	Polymer D	Polymer E	Polymer F
28.64	26.04	28.37	34.33	36.53

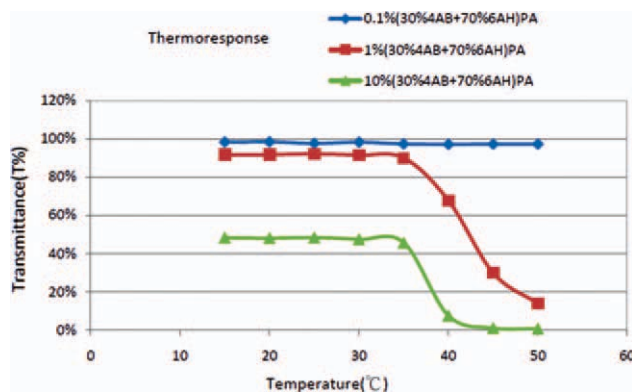


Figure 9 Effect of temperature on UV-Visible transmittance of 1% (w/v) of PBS of polymer B. The measurement was performed at 500 nm from 15 to 50°C. [Color figure can be viewed in the online issue, which is available at wileyonlinelibrary.com.]

mer E, 15% (3.045 mmol) 4AB and 85% (17.255 mmol) 6AH; and polymer F, 10% (2.03 mmol) 4AB and 90% (18.27 mmol) 6AH.

Sample preparation and characterization

Poly(α,β -*N*-substituted-DL-aspartamide)s were added to PBS (1% w/v) under sonication for 10 min to obtain clear solutions. Solutions with different pH values were prepared by adjusting the pH with dilute H₃PO₄ and dilute NaOH solutions, and the phase transition temperature was then determined using a UV-visible (Hitachi U-3300, Japan) spectrophotometer in a temperature-controlled water bath (Firstek). The ¹H-NMR spectra were obtained using a Varian Unity Inova 500 NMR. The molecular weight of the polymers was estimated by gel permeation chromatography (Waters, USA) in DMF containing 20 mmol/L LiBr. The T_g was measured using a DSC (Perkin-Elmer, USA) equipped with

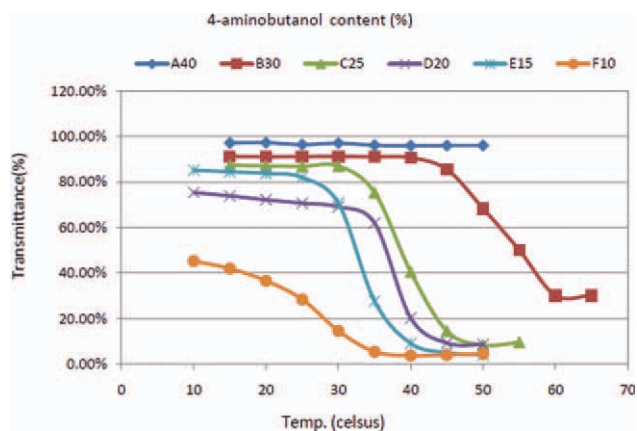


Figure 10 Effect of temperature on light transmittance of 1% (w/v) PBS of polymer (A–F) on the heating process. The measurement was performed at 500 nm. [Color figure can be viewed in the online issue, which is available at wileyonlinelibrary.com.]

TABLE IV
The LCST (°C) of Polymer B–F in 1% (w/v) PBS
Determined by UV–Visible Spectrophotometer

4-aminobutanol content (%)	LCST
30	53
25	40
20	37.5
15	32
10	28

75% ethylene glycol aqueous solution or a liquid nitrogen cooling system. The size and zeta-potential were measured using a Malvern Zetasizer (Nano ZS) at a 1% (w/v) concentration. The pK_a value of each sample was found by acid–base titration of buffer solution. A fluorescence probe was used to determine the critical micelle concentration of the polymers. Transmission electronic microscopy was conducted using a JEOL JEM-2100 (HT). Samples were prepared by dropping 1% sample solution onto 200 mesh carbon-coated copper grid, and then the grids were dried in a vacuum oven at room temperature. Staining of the sample was conducted using 5% phospho-

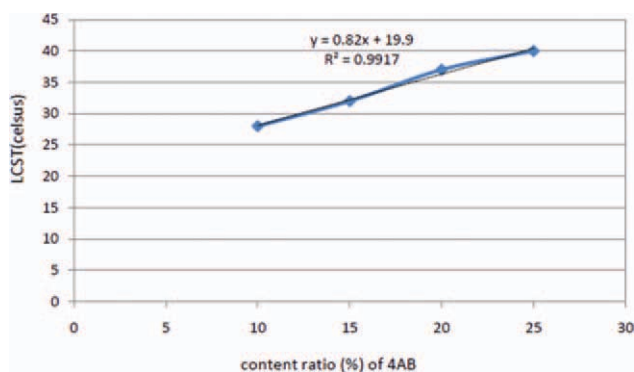


Figure 11 Relationship between content of 3a (4-aminobutanol) in 4(poly(α,β -N-substitute-DL-aspartamide)s and LCST. [Color figure can be viewed in the online issue, which is available at wileyonlinelibrary.com.]

tungstic acid (PTA) solution on a dried grid, and grids expose to PTA were dried in a vacuum oven.

RESULTS AND DISCUSSION

Figures 1 and 2 shows the ^1H NMR and FTIR spectra of PSI prepared by acid-catalyzed bulk thermal

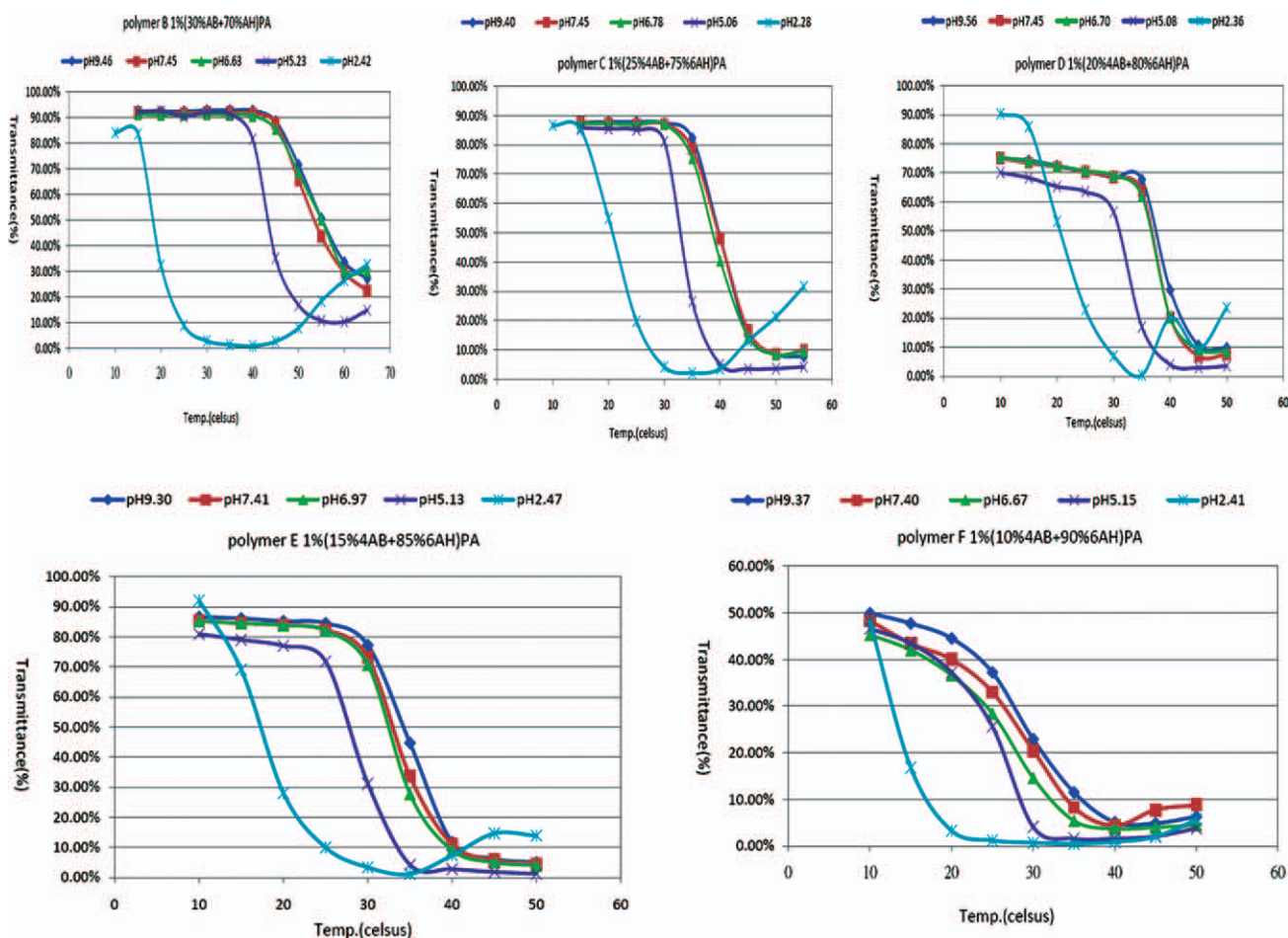


Figure 12 Effect of temperature on light transmittance of 1% (w/v) PBS with different pH of polymer B–F on the heating process. The measurement was performed at 500 nm. [Color figure can be viewed in the online issue, which is available at wileyonlinelibrary.com.]

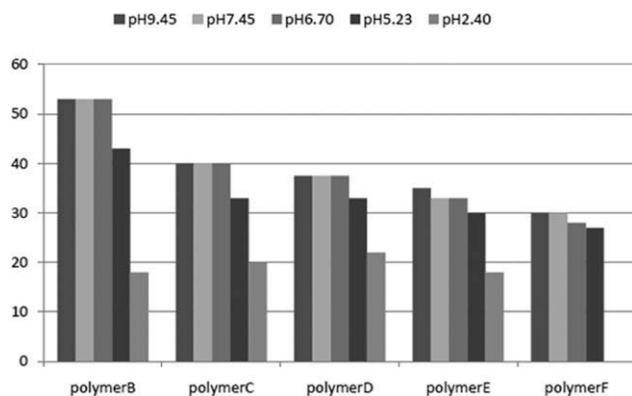


Figure 13 Effect of LCST of different composition ratio of polymer in different pH solution.

polycondensation. The signals at 2.5–2.8 and 3.0–3.3 were assigned to methylene protons, and 5.0–5.4 ppm represents the methine protons of the succinimide repeating units of PSI. The peaks at 6–7 ppm were assigned to the olefin protons of the fumaramic acid end group and the fumaramide units, and the peaks at 8–10 ppm were assigned to the amide protons of the branched and/or opened amide groups, respectively.

The values of M_w , M_n , MP, and PDI of the synthesized PSI were determined by GPC (Table I). Results from the DSC and TGA measurements, including T_g , T_m , ΔH , and decomposition temperature, are given in Table I and Figs. 3–5.

The succinimide units of PSI are easily attacked by 1° amino alcohol to undergo aminolysis. The FTIR spectra (Figs. 2 and 6) of PSI and polymer B showed new bands at 1545 cm^{-1} (amide), 1649 cm^{-1} (amide), and 3100 cm^{-1} (–OH) after aminolysis. From the FTIR spectra, poly (α,β -*N*-substituted-DL-aspartamide)s can be distinguished from PSI.

The chemical structures of the synthesized poly (α,β -*N*-substituted-DL-aspartamide)s was examined by FTIR and $^1\text{H NMR}$ (Figs. 6 and 7). The peaks (Fig. 7) were δ 1.2–1.6 (br, $\text{CH}_2\text{CH}_2\text{CH}_2$), 2.9–3.1 (br, NHCH_2CH_2), 3.3–3.6 (br, $\text{C}(\text{NO})\text{CH}_2\text{CHC}(\text{NO})$), 4.2–4.8 (br, $\text{C}(\text{NO})\text{CH}_2\text{CHC}(\text{NO})$, CH_2OH), 7.5–8.5 (br, NH). The grafting ratio of 1° amino alcohol to PSI was 100% as determined using the peaks at 5.0–5.4 ppm (Fig. 1) and 4.2–4.8 ppm (Fig. 7). The peak at 5.0–5.4 ppm disappeared after grafting (Fig. 7).

TABLE V
The LCST (°C) of Polymer B–F in Different pH Determined by UV–Visible Spectrophotometer

pH	Polymer B	Polymer C	Polymer D	Polymer E	Polymer F
9.45	53	40	37.5	35	30
7.45	53	40	37.5	33	30
6.70	53	40	37.5	32	28
5.23	43	33	33	30	27
2.40	18	20	20	27	13

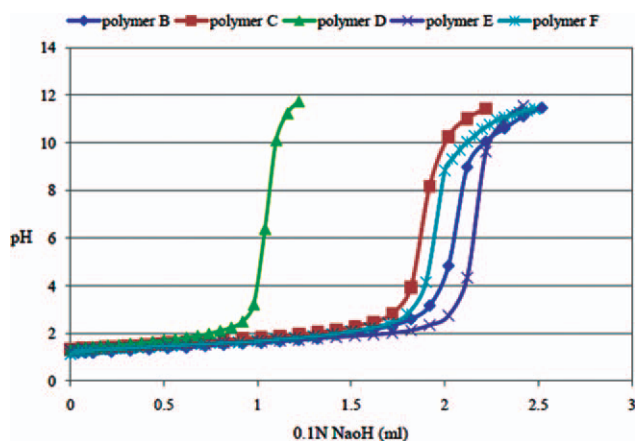


Figure 14 The result of acid–base titration of 1% (w/v) polymer solution in 0.1N HCl, titrated with 0.1N NaOH, pK_a value could be found from the midpoint of straight line of each curve. [Color figure can be viewed in the online issue, which is available at wileyonlinelibrary.com.]

The values of M_w , M_n , MP, and PDI of the final synthesized poly (α,β -*N*-substituted-DL-aspartamide)s were determined by GPC (Table II). The glass transition temperatures (T_g) of polymers B–F are shown in Figure 8 and Table III. These data indicate that polymers B–F would be in a rubber-like state at body temperature ($36.5\text{--}37.5^\circ\text{C}$).

Figure 9 shows the temperature dependence of the light transmittance of poly (30% 4AB + 70% 6AH) aspartamide (polymer B) in PBS at different concentrations at 500 nm during the heating process. The turbidity of 10% and 1% polymer B showed drastic changes during the heating process, with the transmittance decreasing markedly around the transition temperature (LCST); however, the light transmittance of 0.1% polymer B did not change, indicating that the 0.1% concentration (w/v) was below the critical aggregate concentration for the phase transition. The LCST of the 10% polymer solution was 38°C , lower than the LCST of the 1% polymer B, which was 42°C . Solutions with higher concentrations typically have lower LCSTs in this type of system.

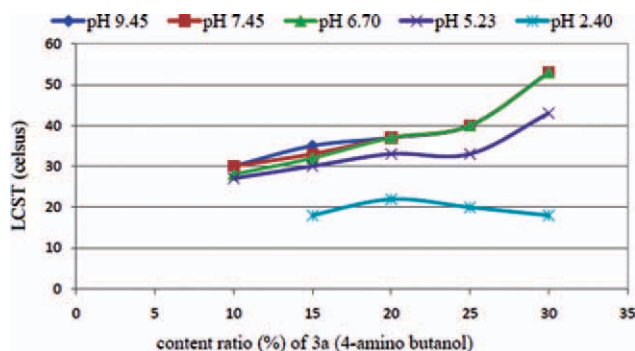


Figure 15 LCST of 1% (w/v) poly (α,β -*N*-substituted-DL-aspartamide)s, in PBS solutions with different 4AB/6AH ratios at different pH. [Color figure can be viewed in the online issue, which is available at wileyonlinelibrary.com.]

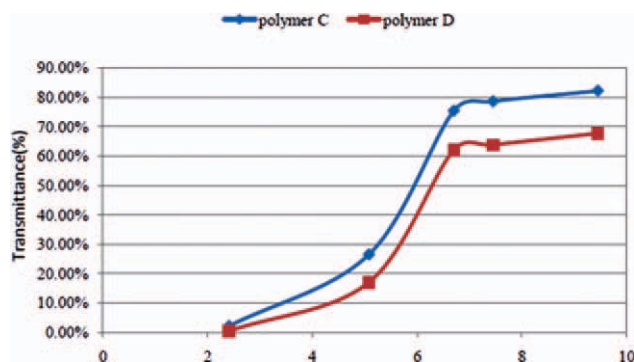


Figure 16 Effect of pH on transmittance (500 nm) of 1% (w/v) aqueous solution of polymer C and D at 35°C. [Color figure can be viewed in the online issue, which is available at wileyonlinelibrary.com.]

Figure 10 illustrates the phase transition of poly(α,β -*N*-substituted-DL-aspartamide)s (polymers B–F) prepared at a concentration of 1% (w/v) in PBS, and data that represent lower critical solution temperatures (LCSTs) are presented in Table IV. The phase transition phenomena result from changes in solubility; i.e., polymers aggregate or disperse based on the interactions of the molecular forces at temperatures. Different composition ratios of 4AB and 6AH (polymers A–F) produce different phase transition temperatures (10–65°C). The LCST increases as the ratio of more hydrophilic component, 4AB increases (see Fig. 11). However, polymer A does not exhibit phase transition phenomenon and does not have an LCST. The LCSTs of polymers B, C, D, E, and F are 53, 40, 36, 32, and 28°C, respectively.

The phase transition temperature of polymers B–F is affected by the pH of their aqueous environment: the LCST decreases as the pH decreases (see Figs. 12 and 13 and Table V). However, between pH 9.40 and 6.70, the LCSTs of polymers B–F did not change much because of the limited changes in the ionization of the polymers at alkaline to neutral pHs. The pK_a values of polymer B–F were all at 7.0 (Fig. 14). A general trend of increasing LCST with increasing 4AB, as seen from Figure 15, was observed, the only exception being at pH 2.4. The LCST decreases when the percentage of 4AB increases from 20 to 30%. This peculiar phenomenon is due to the fact that the pK_a of poly(α,β -*N*-substituted-DL-aspartamide)s which are 7.0 is much higher than pH 2.4, resulting in lot of lack of ionization and reducing the solubility. Therefore, at pH 2.4, the composition ratio of 3a (hydrophilic) is higher; conversely, the solubility is lower. The effect of pH on the transmittance of the polymeric solutions was determined at 35°C using polymers C and D (Fig. 16). A clear phase transition existed at roughly pH 6.7 and 7.45, respectively. On the basis of the Henderson-Hasselbalch equation, as the pH values are higher than pK_a , samples tend toward ionic phase, and it means

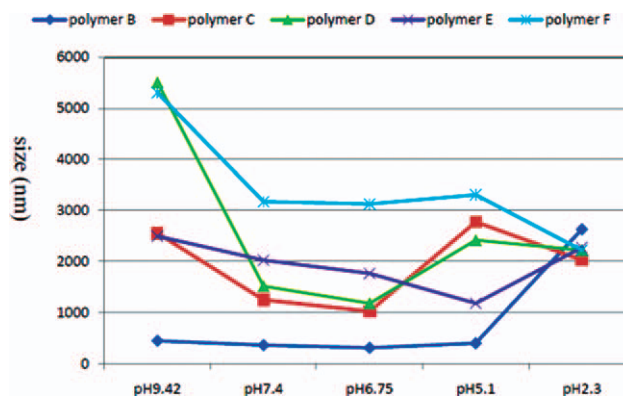


Figure 17 Size of polymer B–F 1% (w/v) in PBS with different pH determined by Malvern Zetasizer at 25°C. Note: The particle size range of Malvern Zetasizer is 0.6 nm–6 μ m. [Color figure can be viewed in the online issue, which is available at wileyonlinelibrary.com.]

the dissolution of samples rise. These experimental data clearly demonstrate the pH sensitivity of polymers C and D. Figure 17 shows the changes in the size of the aggregates in 1% (w/v) solutions of polymers B to F in PBS in response to the pH change. The zeta-potential of the polymeric particles (see Table VI) can also explain this pH sensitivity. As the solution is alkalized, electrostatic repulsion becomes stronger due to the increasing negative charge (hydroxyl groups) and leads to the distance between aggregates becomes longer (Fig. 18). The behavior explains why the size determined by DLS is so large but the transmittance measured by UV–visible spectrophotometer is high. Conversely, the charges on the polymers are all close to zero in strongly acidic solutions; thus the electrostatic repulsion force disappears, resulting in the coalescing of the polymers into larger aggregates, in contrast to the behavior in weakly acidic, neutral and alkaline solutions. In brief, the electrostatic repulsion weakens at acidic pH, the polymeric species collapse and form larger aggregates, and the solutions become turbid.

The nature and the morphology of the micelles we observed were elucidated by SEM and TEM. The micelles were in the form of unilamellar bilayer polymersomes.^{69,70} The samples were prepared with 1%

TABLE VI
Zeta-Potential of Polymer B–F 1% (w/v) in PBS with Different pH Determined by Malvern Zetasizer at 25°C

pH	Polymer B	Polymer C	Polymer D	Polymer E	Polymer F
9.45	−15	−13.5	−10.5	−11.3	−10.8
7.45	−11.3	−9.6	−7.5	−7.4	−11.3
6.75	−6.9	−7.1	−6.9	−7.5	−9.5
5.06	−4.9	−5.4	−6.1	−6.9	−7.3
2.20	−1.39	−2.46	−1.65	−0.676	−1.89

The size range for zeta-potential of Malvern Zetasizer is 5 nm–10 μ m.

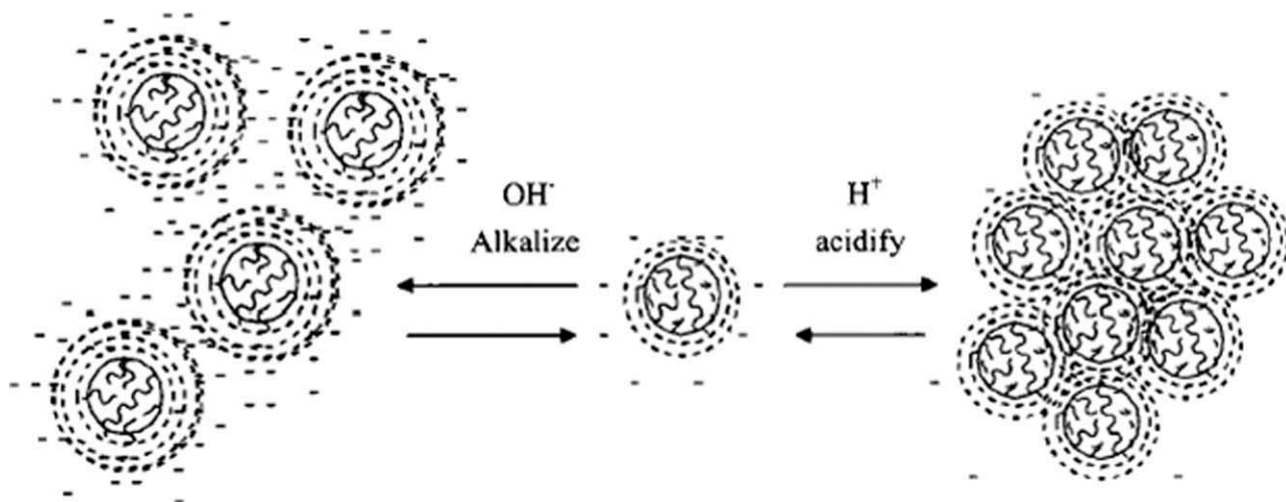


Figure 18 The scheme of zeta-potential and size change of 1% (w/v) polymer B-F in PBS respond to the pH change.

(w/v) polymer B and D in PBS. Many vesicle-like hollow micelles were clearly identified by SEM (see Fig. 19), and the diameters of polymersomes were $\sim 0.5\text{--}1\ \mu\text{m}$, which is in agreement with the size measurements. TEM images (Fig. 20) clearly show the morphologies of the self-assembled vesicles prepared and indicate the formation of unilamellar polymersomes with bilayer structures. The amides and saturated hydrocarbons of the polymers were negatively stained by PTA; therefore, the dark circle of the shell can be directly observed. The amide groups form the backbone of poly (α,β -*N*-substituted-DL-aspartamide)s.

Figures S1–S5 (see Supporting Information) and Table VII show the diagrams for all series of poly (α,β -*N*-substituted-DL-aspartamide)s and the CMC values for all samples. All log *C* values of the CMCs were between 0 and 1.5, and were 10 times higher than those of most other polymeric micelles, which

are typically in the range of -2 to 3 of log *C*. The trend for the CMC can be observed from Table VII; the CMC decreased along with increasing content of hydrophilic 4-aminobutanol chains. Because the crucial factor in the formation of polymersome is the hydrophilic interaction not the hydrophobic interaction, more hydrophiles are conducive to form polymersomes.

CONCLUSIONS

In this study, a series of novel polymers were characterized, the intermediate, PSI and poly(α,β -*N*-substituted-DL-aspartamide)s were successfully synthesized by acid-catalyzed bulk thermal polycondensation of L-aspartic acid and aminolysis with the 1° amino alcohol, 4-aminobutanol, and 6-aminohexanol. The compositions, physical properties, and molecular weights

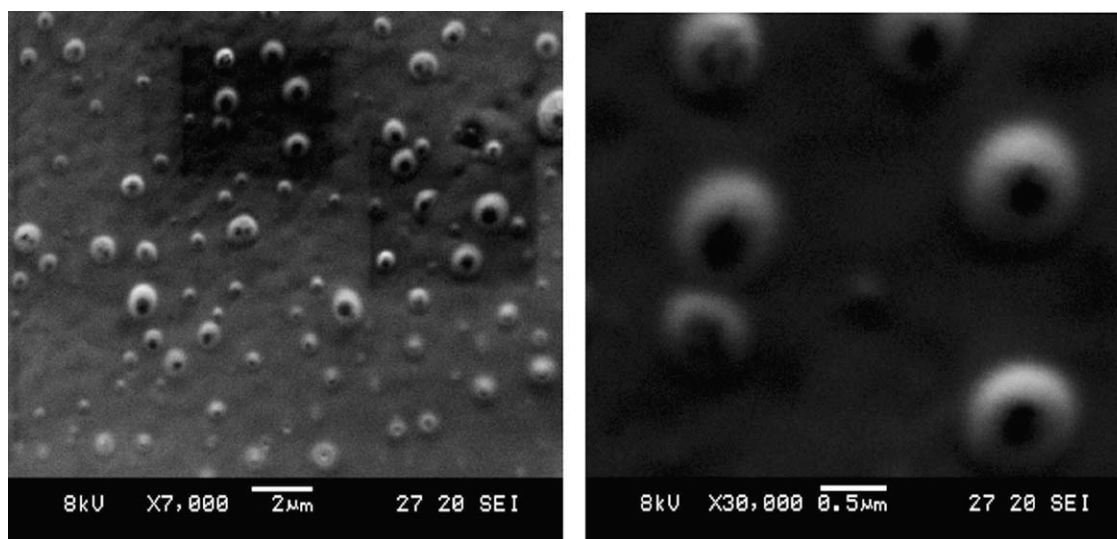
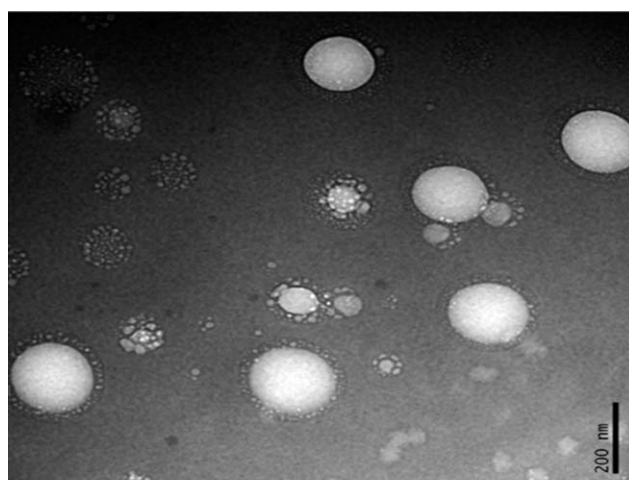
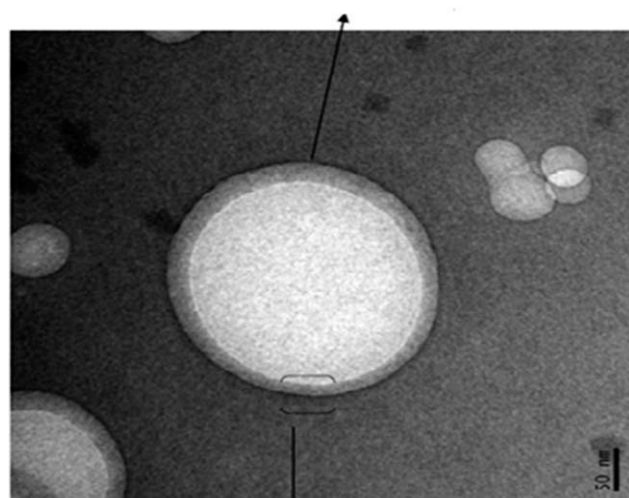


Figure 19 SEM micrograph of polymer B with vesicle-like microparticles (polymersome) prepared by 1% (w/v) in PBS.



Amide G. and saturated hydrocarbon G. stained by PTA



Vesicle shell layer (10-20 nm in thickness)

Figure 20 TEM image of polymerosomes of polymer B and D prepared by 1% (w/v) in PBS negatively stained with phosphotungstic acid solution (5% w/v).

of PSI and poly(α,β -*N*-substituted-DL-aspartamide)s were determined by ^1H NMR, FTIR, FL, DSC, and GPC. The poly(α,β -*N*-substituted-DL-aspartamide)s showed pH and temperature responsiveness and had phase transitions at different pHs and temperatures. As the composition ratio of hydrophilic 4AB increased, the LCST increased. Poly(α,β -*N*-substi-

tuted-DL-aspartamide)s in alkaline and neutral aqueous solutions tended to remain dispersion, whereas these polymers began to aggregate in weakly acidic solutions and congregated hugely in strongly acidic state. Furthermore, the LCSTs of the polymers decreased as the pH decreased below neutral. Finally, these pH- and thermo-responsive polymers can be used as potential candidates to apply in drug delivery systems and in the biomedical field. The proceeding Lab. work is going to demonstrate the characteristics of self-assembly in aqueous solution and the LCST can be applied in drugs that are water-soluble or amphiphilic but a have short 12 circulation half-life to achieve the goal of prolonging drug release in the body.

References

1. Kikuchi, A.; Okano, T. *Prog Polym Sci* 2002, 27, 1165.
2. Zhang, J.; Peppas, N. A. *Macromolecules* 2000, 33, 102.
3. Furth, M. E.; Atala, A.; Van Dyke, M. E. *Biomaterials* 2007, 28, 5068.
4. Izumi, A.; Nomura, R.; Masuda, T. *Macromolecules* 2001, 34, 4342.
5. Simitzis, J.; Triantou, D.; Soulis, S. *J Appl Polym Sci* 2010, 118, 1494.
6. Akira, M.; Syuhei, I.; Atsushi, H.; Kazunori, K. *Biomacromolecules* 2003, 4, 1410.
7. Hirokawa, Y.; Tanaka, T. *J Chem Phys* 1984, 81, 6379.
8. Chang, Y.; Bender, J. D.; Phelps, M. V. B.; Allcock H. R. *Biomacromolecules* 2002, 3, 1364.
9. Peng, K. T.; Chen, C. F.; Chu, I. M.; Li, Y. M.; Hsu, W. H.; Hsu, R. W. W.; Chang, P. J. *Biomaterial* 2010, 31, 5227.
10. Samarth, K.; Christine, S.; Boris, G.; Muller, A. H. E.; Hoffman, A. S.; Stayton, P. S. *Biomacromolecules* 2006, 7, 2736.
11. Overstreet, D. J.; Dhuv, H. D.; Vernon, B. *Biomacromolecules* 2010, 11, 1154.
12. Lee, A. S.; Butun, V.; Vamvakaki, M.; Armes, S. P.; Pople, J. A.; Gast, A. P. *Macromolecule* 2002, 35, 8540.
13. Maria, A. C.; Giovanna, P.; Rossella, C.; Patrizia, P.; Gaetano, G. *Biomacromolecules* 2008, 9, 43.
14. Galaev, I. Y.; Mattiasson, B. *Trends Biotechnol* 1999, 17, 335.
15. Hoffman, A. S. *J Biomed Mater Res* 2000, 52, 577.
16. Jeong, B.; Gutowska, A. *Trends Biotechnol* 2002, 20, 305.
17. Schmaljohann, D. *Adv Drug Deliv Rev* 2006, 5, 1655.
18. Gil, E. S.; Hudson, S. M. *Prog Polym Sci* 2004, 29, 1173.
19. Alarcon, C. D. H.; Pennadam, S.; Alexander, C. *Chem Soc Rev* 2005, 34, 276.
20. Tsai, H. C.; Chang, W. H.; Lo, C. L.; Tsai, C. H.; Chang, C. H.; Ou, T. W.; Yen, T. C.; Hsiue, G. H. *Biomaterials* 2010, 31, 2293.
21. Gillies, E. R.; Jonsson, T. B.; Frechet, J. M. *J Am Chem Soc* 2004, 126, 11936.
22. Li, G. Y.; Shi, L. Q.; Ma, R. J.; An, Y. L.; Huang, N. *Angew Chem Int Ed* 2006, 45, 4959.
23. Gan, L. H.; Gan, Y. Y.; Deen, G. R. *Macromolecules* 2000, 33, 7893.
24. Bulmus, V.; Ding, Z.; Long, C. J.; Stayton, P. S.; Hoffman, A. S. *Bioconjugate Chem* 2000, 11, 78.
25. Lo, C. L.; Huang, C. K.; Lin, K. M.; Hsiue, G. H. *Biomaterials* 2007, 28, 1225.
26. Yin, X.; Stover, H. D. H. *Macromolecules* 2002, 35, 10178.
27. Valeria, A.; Orietta, M.; Daniele, N.; Jose, M. K.; Albert, M. *Biomacromolecules* 2009, 10, 2672.
28. Jeong, B.; Lim, S. W.; Bae, T. H. *Adv Drug Deliv Rev* 2002, 54, 37.

TABLE VII
Critical Micelle Concentration (mg/mL) Organized from Fig. S1-S5

Sample name	Critical micelle concentration
Polymer B (30% AB + 70% AH) PA	0.02998
Polymer C (25% AB + 75% AH) PA	0.05525
Polymer D (20% AB + 80% AH) PA	0.0859
Polymer E (15% AB + 85% AH) PA	0.14424
Polymer F (10% AB + 90% AH) PA	0.7651

29. Yukio, N.; Fumiaki, M.; Masao, K.; Hidetoshi, A.; Takashi, T. *Macromolecules* 1996, 29, 5859.
30. Suda, K.; Wada, Y.; Kikunaga, Y.; Morishita, K.; Kishida, M. *J Polym Sci Part A: Polym Chem* 1997, 35, 1763.
31. Lee, B. H.; Lee, Y. M.; Sohn, Y. S.; Song, S. C. *Macromolecules* 2002, 35, 3876.
32. Chang, Y.; Powell, E. S.; Allock, H. R.; Park, S. M.; Kim, C. *Macromolecules* 2003, 36, 2568.
33. Taylor, L. D.; Cerankowski, L. D. *J Polym Sci Part A: Polym Chem* 1975, 13, 2551.
34. Schild, H. G. *Prog Polym Sci* 1992, 17, 163.
35. Fujishige, S.; Kubota, K.; Ando, I. *J Phys Chem* 1989, 93, 3311.
36. Kubota, K.; Fujishige, S.; Ando, I. *J Phys Chem* 1990, 94, 5154.
37. Inomate, H.; Goto, S.; Saito, S. *Macromolecules* 1990, 23, 4887.
38. Katsuto, O.; Inomata, H.; Goto, S.; Saito, S. *Macromolecules* 1990, 2, 283.
39. Kisselev, A. M.; Manias, E. *Fluid Phase Equilib* 2007, 261, 69.
40. Winnik, F. M. *Macromolecules* 1990, 23, 233.
41. Bromberg, L. E.; Ron, E. S.; Ron, E. S. *Adv Drug Delivery Rev* 1998, 31, 197.
42. Kujawa, P.; Winnik, F. M. *Macromolecules* 2001, 43, 4310.
43. Torres-Lugo, M.; Peppas, N. A. *Macromolecules* 1999, 32, 6646.
44. Philippova, O. E.; Hourdet, D.; Audebert, R.; Khokhlov, A. R. *Macromolecules* 1997, 30, 8278.
45. Lee, E.; Shin, H.; Na, K.; Bae, Y. *J Controlled Release* 2003, 90, 363.
46. Luo, L.; Kato, M.; Tsuruta, T.; Kataoka, K.; Nagasaki, U. *Macromolecules* 2002, 33, 4992.
47. Shen, H. W.; Zhang, L. F.; Eisenberg, A. *J Am Chem Soc* 1999, 12, 2727.
48. Lee, A.; Buetem, V.; Vamvakaki, M.; Armes, S. P.; Pople, J.; Gast, A. *Macromolecules* 2002, 35, 8540.
49. Lee, E.; Na, K.; Bae, Y. *Nano Lett* 2005, 5, 325.
50. Claude, A.; Hoarau, C.; Leroux, J. C. *Biomacromolecules* 2004, 5, 2082.
51. Zhang, X.; Li, J.; Li, W.; Zhang, A. *Biomacromolecules* 2007, 8, 3557.
52. Tachibana, Y.; Kurisawa, M.; Uyama, H.; Kobayashi, S. *Biomacromolecules* 2003, 4, 1132.
53. Tachibana, Y.; Kurisawa, M.; Uyama, H.; Kobayashi, S. *Chem Commun* 2003, 1, 106.
54. Nakato, T.; Oda, K.; Yoshitake, M.; Tomida, M. *J Macromol Sci Part A: Pure Appl Chem* 1999, 36, 949.
55. Watanabe, E.; Tomoshige, N.; Uyama, H. *Macromol Symp* 2007, 249/250, 509.
56. Neri, P.; Antoni, G.; Benvenuti, F.; Cocola, F.; Gazzai, J. G. *J Med Chem* 1973, 16, 893.
57. Cheng, J.; Teply, B. A.; Sherifi, I.; Sung, J.; Luther, G.; Gu, F. X.; Etgar, L. V.; Aleksandar, F. R. M.; Langer, R.; Farokhzad, O. C. *Biomaterials* 2007, 28, 869.
58. Lin, Y. H.; Chung, C. K.; Cheng, C. T.; Liang, H. F.; Cheng, S. H.; Sung, H. W. *Biomacromolecules* 2005, 6, 1104.
59. Kim, H. J.; Ishii, A.; Miyata, K.; Lee, Y.; Wu, S.; Oba, M.; Nishiyama, N.; Kataoka, K. *J Controlled Release* 2010, 145, 141.
60. Cheng, H.; Li, Y. Y.; Zeng, X.; Sun, Y. X.; Zhang, X. Z.; Zhuo, R. X. *Biomaterials* 2009, 30, 1246.
61. Thombre, S. M.; Sarwade, B. D. *J Macromol Sci Part A: Pure Appl Chem* 2005, 42, 1299.
62. Yang, J.; Wang, F.; Fang, L.; Tan, T. W. *Environ Pollut* 2007, 149, 125.
63. Zhang, W.; Huang, J.; Fan, N.; Yu, J.; Liu, Y.; Liu, S.; Wang, D.; Li, Y. *Coll Surf B: Biointerface* 2010, 81, 297.
64. Obst, M.; Steinbuechel, A. *Biomacromolecules* 2004, 5, 1166.
65. Richard, A. G.; Bhanu, K. *Science* 2002, 297, 803.
66. Nariyoshi, K.; Hidetaka, H.; Hidetoshi, O. *J Ferment Bioeng* 1995, 79, 317.
67. Takeshi, N.; Masako, Y.; Koshi, M.; Masayuki, T. *Macromolecules* 1998, 31, 2107.
68. Nakato, T.; Kusuno, A.; Kakuchi, T. *J Polym Sci Part A: Polym Chem* 2000, 38, 117.
69. Lee, H. J.; Yang, S. R.; An, E. J.; Kim, J. D. *Macromolecules* 2006, 39, 4938.
70. Zheng, C.; Qiu, L.; Zhu, K. *Polymer* 2009, 50, 1173.